Toward a Total Model for the Molybdenum Hydroxylases: Synthesis, Redox, and Biomimetic Chemistry of Oxo-thio-Mo(VI) and -Mo(V) Complexes

Paul D. Smith,[1a] Damian A. Slizys,[1a] Graham N. George,[1b] and Charles G. Young*,[1a]

School of Chemistry, University of Melbourne Victoria 3010, Australia
Stanford Synchrotron Radiation Laboratory, SLAC Stanford University, P.O. Box 4349, MS 69 Stanford, CA 94309

Received October 28, 1999

Development of a total synthetic model for the molybdenum hydroxylases, which feature mononuclear oxo-thio-Mo(VI), Mo(V), and Mo(IV) centers during turnover, has been hampered by the instability of $[Mo^{VI}OS]^{2+}$ complexes and their reduced counterparts.[2−5] We have approached the synthesis of stable, cleanly-reduced $[Mo^{VI}OS]^{2+}$ species[6] by fine-tuning the redox properties of L^xMoOSX [L^x = hydrotris(3,5-dimethylpyrazol-1-yl)borate (L), hydrotris(3-isopropylpyrazol-1-yl)borate (L^{Pr})] complexes, through variation of the co-ligand X, to reduce the susceptibility of the Mo^{VI}═S unit towards internal redox.[7−9] Here, we describe the first hydroxylase model to feature interconvertible $[Mo^{VI}OS]^{2+}$, $[Mo^{V}OS]^{+}$, and $[Mo^{V}O(SH)]^{2+}$ complexes having common co-ligands (L^{Pr} and X = OPh^-) and structural, spectroscopic, and chemical properties relevant to the biological systems.

Reaction of orange $L^{Pr}MoO_2(OPh)$[9] with PEt_3 in acetonitrile results in the formation of green $L^{Pr}MoO(OPh)(OPEt_3)$, which reacts with propylene sulfide to generate the red-brown, oxo-thio-Mo(VI) complex, $L^{Pr}MoOS(OPh)$ (**1**). Aerobic chromatographic workup of the reaction results in the isolation of brown-purple $[L^{Pr}MoO]_2(\mu\text{-}O)(\mu\text{-}S_2)$, which is closely related to $[LMoO]_2(\mu\text{-}O)(\mu\text{-}S_2)$[10] formed upon aerial oxidation of $[LMoOSX]^-$ complexes.[9,10] The formation of $[L^xMoO]_2(\mu\text{-}O)(\mu\text{-}S_2)$ from L^xMoOSX is interpreted in terms of the two-step process in eq 1.

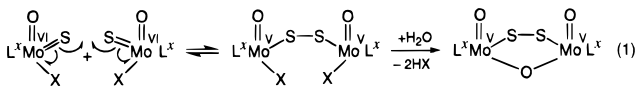

(1)

Anaerobic workup of the reaction yields a major red-brown fraction containing **1**.[11] However, to date, only a dimeric μ-disulfido-Mo(V) "modification", viz., black-brown $[L^{Pr}MoOS(OPh)]_2$ (**2**), has been structurally characterized.[12] Centrosymmetric **2** (Figure 1) is comprised of two 6-coordinate, distorted octahedral Mo centers bridged by a μ-disulfido-κS:$\kappa S'$ ligand. The Mo−O(1) distance of 1.674(3) Å is typical of terminal Mo═O bonds, while the Mo−S distance of 2.3244(11) Å is characteristic of an Mo−S single bond.[13] The S−S′ distance of 2.095(2) Å is consistent with the presence of an S−S single bond.[13] The Mo−N(n1) distances decrease in the order Mo−N(11) > Mo−N(21) > Mo−N(31), consistent with ligand *trans* influences in the order oxo > disulfido > phenolate. While **2** represents a nascent state of **1**, there is evidence for the independent existence of **1** in the solid state.[14]

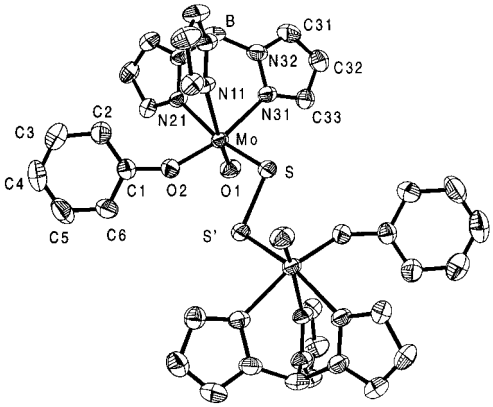

Figure 1. Structure of **2** (iso-propyl groups and hydrogen atoms omitted, numbering scheme as per pyrazole ring 3). Additional bond lengths (Å) and angles (deg): Mo−O(2) 1.927(3), Mo−N(11) 2.396(3), Mo−N(21) 2.226(3), Mo−N(31) 2.191(3), O(1)−Mo−O(2) 103.36(13), O(1)−Mo−S 101.38(10), O(2)−Mo−S 91.93(8), Mo−S−S′ 103.47(7), Mo−O(2)−C(1) 142.9(2).

In any case, the S−S bond of dimeric **2** is cleaved to form **1** upon dissolution in acetonitrile, chloroform, dichloromethane, or toluene.[11] In the first three solvents, ESI-MS reveals a dominant peak cluster at m/z 601 ([**1** + Na]$^+$), and in dichloromethane osmometric measurements established a molecular mass of 594 ± 30. ^{1}H NMR spectra were indicative of molecular C_1 symmetry and the presence of a diamagnetic species in $CDCl_3$. Solution IR

(1) (a) University of Melbourne. (b) Stanford Linear Accelerator Center.

(2) Hille, R. *Chem. Rev.* **1996**, *96*, 2757−2816.

(3) (a) Pilato, R. S.; Stiefel, E. I. In *Inorganic Catalysis*, 2nd ed.; Reedijk, J., Bouwman, E., Eds.; Marcel Dekker: New York, 1999; p 81−152. (b) Enemark, J. H.; Young, C. G. *Adv. Inorg. Chem.* **1993**, *40*, 1−88. (c) Young, C. G. *J. Biol. Inorg. Chem.* **1997**, *2*, 810−816.

(4) For known $[Mo^{VI}OS]^{2+}$ complexes see: Thapper, A.; Donahue, J. P.; Musgrave, K. B.; Willer, M. W.; Nordlander, E.; Hedman, B.; Hodgson, K. O.; Holm, R. H. *Inorg. Chem.* **1999**, *38*, 4104−4114 and refs 2 and 3.

(5) The "Very Rapid" and "Rapid" EPR-active enzyme states are assigned to oxo-thio-Mo(V) and oxo(hydrosulfido)-Mo(V) centers, respectively. See Bray, R. C. *Q. Rev. Biophys.* **1988**, *21*, 299−329 and refs 2 and 3.

(6) Stable $LMo^{VI}OS(S_2PPr^i{}_2\text{-}S)$ has a Mo(V) counterpart but features an intramolecular Mo═S···S interaction absent in the enzymes. Eagle, A. A.; Laughlin, L. J.; Young, C. G.; Tiekink, E. R. T. *J. Am. Chem. Soc.* **1992**, *114*, 9195−9197.

(7) It is possible to *estimate* the reduction potentials of L^xMoOSX complexes by assuming they are ∼400 mV more positive than those of their dioxo analogues.[8,9] Oxo-thio-Mo(VI) complexes with large negative reduction potentials, viz. X = EPh and ER_{alkyl} (E = O, S) derivatives, are more likely to be stable with respect to internal redox.

(8) For comparative electrochemical studies see: (a) Bristow, S.; Collison, D.; Garner, C. D.; Clegg, W. *J. Chem. Soc., Dalton Trans.* **1984**, 1617−1619. (b) Eagle, A. A.; Harben, S. M.; Tiekink, E. R. T.; Young, C. G. *J. Am. Chem. Soc.* **1994**, *116*, 9749−9750.

(9) Xiao, Z.; Bruck, M. A.; Doyle, C.; Enemark, J. H.; Grittini, C.; Gable, R. W.; Wedd, A. G.; Young, C. G. *Inorg. Chem.* **1995**, *34*, 5950−5962.

(10) Xiao, Z.; Enemark, J. H.; Wedd, A. G.; Young, C. G. *Inorg. Chem.* **1994**, *33*, 3438−3441. The compound is also isolated (via eq 1) after aerobic workup of reactions of LMoOX (X = cysteine-OMe, $SCH_2CH_2NH_2$, and $S_2P(OEt)_2$) with propylene sulfide (unpublished results).

(11) Procedures were performed anaerobically. A solution of $L^{Pr}MoO_2(OPh)$[9] (562 mg, 1 mmol) and triethylphosphine (0.22 mL, 1.5 mmol) in acetonitrile (30 mL) was stirred for 15 h. Propylene sulfide (0.8 mL, 10 mmol) was then added, and the mixture was stirred for a further 2 h. The solvent was removed in vacuo and the residue was column chromatographed on silica-CH_2Cl_2/hexanes (2:3). The red-brown fraction was concentrated to ∼5 mL and cooled at −8 °C for ∼15 h. Black-brown **2** was collected, washed with hexanes (2 × 5 mL), and dried in vacuo. Yield 453 mg, 78%. Anal. Calcd for $C_{48}H_{66}B_2Mo_2N_{12}O_4S_2$: C, 50.01; H, 5.77; N, 14.58; S, 5.56. Found: C, 50.31; H, 5.93; N, 14.49; S, 5.51. IR (cm^{-1}) KBr, ν(BH) 2473, 2450 m, ν(OPh) 1588 m, ν(CN) 1507 s, ν(MoO) 940 s. For **1** (solutions of **2**): IR (cm^{-1}) CH_2Cl_2, ν(MoO) 914 s, ν(MoS) 483 s; $CHCl_3$, 917 s, 483 s; toluene, 916 m, 481 s. UV/vis, λ/nm (ϵ/M^{-1} cm^{-1}) CH_2Cl_2, 503 (696); toluene, 503 (723). ^{1}H NMR ($CDCl_3$) δ 0.89, 0.99, 1.18, 1.22, 1.26, 1.31 (d, 3H, 6 CH_3 of L^{Pr}), 3.07, 3.7, 4.62 (sept, 1H, 3 CH of L^{Pr}), 5.98, 6.16, 6.19 (d, 1H, 3 CH of L^{Pr}), 7.01 (t, 1H, OPh), 7.13 (d, 2H, OPh), 7.33 (t, 2H, OPh), 7.54, 7.68, 7.68 (d, 1H, 3 CH of L^{Pr}). ESI-MS (toluene) m/z 601 ([**1** + Na]$^+$, 78%). Molecular mass (osmometry, CH_2Cl_2), 594 ± 30. Echem. (MeCN) $E_{1/2}$ −0.48 V vs SCE (ΔE_{pp} 68 mV, I_{pa}/I_{pc} 0.98).

(12) Crystals of **2** were obtained from CH_2Cl_2/hexanes via slow diffusion. Crystallographic data: $C_{48}H_{66}B_2Mo_2N_{12}O_4S_2$, fw 1152.74, monoclinic space group $P2_1/n$ with a = 15.354(2) Å, b = 11.845(3) Å, c = 16.681(2) Å, β = 116.702(11)°, V = 2710.3(8) Å^3, and D_c = 1.413 g.cm^{-3} for Z = 2. A total of 4770 unique data with 3352 reflections having $I > 2\sigma(I)$ were collected. Refinement on F^2 converged with R_1 0.0428 and wR_2 0.0724.

(13) Orpen, A. G.; Brammer, L.; Allen, F. H.; Kennard, O.; Watson, D. G.; Taylor, R. *J. Chem. Soc., Dalton Trans.* **1989**, S1−S83.

(14) The IR spectrum of **2** sometimes exhibited additional bands, at 917 and 483 cm^{-1}, assigned to the monomer. Trace monomer is also evident (at 2466 eV) in the S K-edge XAS of the solid (Figure 2).

10.1021/ja9938332 CCC: $19.00
Published on Web 03/14/2000

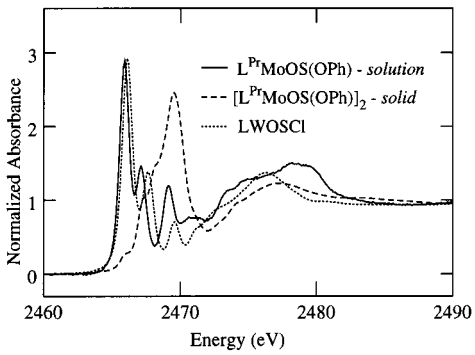

Figure 2. Sulfur K-edge X-ray absorption spectra of solid **2**, a toluene solution of **1**, and solid LWOSCl (all at 293 K).

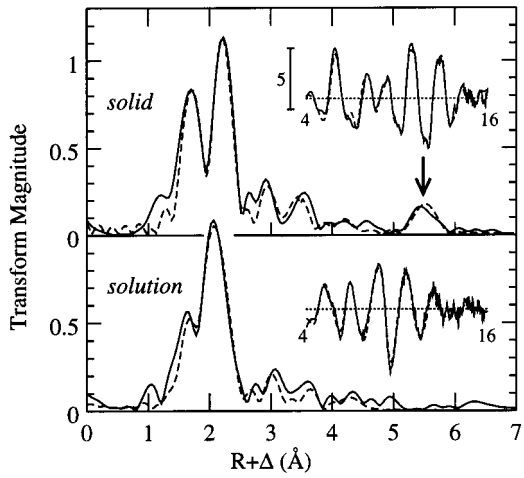

Figure 3. Molybdenum K-edge EXAFS Fourier transforms of solid **2** (top) and a toluene solution of **1** (bottom), with the raw (k^3 weighted) EXAFS shown in the insets. Solid lines show experimental data, while broken lines show the best fits obtained.[15]

spectra[11] reveal strong bands at 917 and 483 cm^{-1} which are assigned to the ν(Mo═O) and ν(Mo═S) vibrational modes, respectively, of **1**.[14] The cyclic voltammogram of **1** in acetonitrile/0.2 M $NBu^n_4BF_4$ exhibits a reversible one-electron reduction at −0.48 V vs SCE, consistent with the reduction of a monomeric species rather than a μ-disulfido dimer.

Sulfur and molybdenum K-edge X-ray absorption spectra (XAS) provide convincing evidence for the presence of **1** in toluene. As shown in Figure 2, the solid state and toluene solution S K-edge XAS are radically different, the latter exhibiting a pre-edge feature characteristic of an oxo-thio-metal fragment; cf. the S K-edge XAS of **1** in toluene and solid LWOSCl.[8b] The strong pre-edge feature arises from a dipole-allowed transition from the S 1s orbital to the Mo═S π* orbital. The pre-edge feature is almost totally absent from the S K-edge XAS of the solid, comprised principally of **2**. Molybdenum K-edge extended X-ray absorption fine structure (EXAFS) studies (Figure 3) support these findings.[15] For the solid, EXAFS analysis reveals Mo═O and Mo−S interactions at 1.68 and 2.32 Å, respectively, along with an Mo···Mo backscattering feature at 5.6 Å (arrowed in Figure 3), consistent with the values determined by X-ray crystallography. In contrast, the very different EXAFS from the toluene frozen solution (containing **1**) reveals short Mo═O and Mo═S interactions of 1.69 and 2.15 Å, respectively. There is no evidence of backscattering from a neighboring Mo atom. In summary "L^{Pr}-MoOS(OPh)" exists in two forms, **1** and **2**, related by an exquisitely poised redox equilibrium (step 1, eq 1).

Electrochemical or chemical (NBu^n_4SH or $CoCp_2$) reduction of **1** results in the formation of the pink-orange oxo-thio-Mo(V) anion, $[L^{Pr}MoOS(OPh)]^-$, which is protonated by adventitious water to form the oxo(hydrosulfido)-Mo(V) complex, $L^{Pr}MoO(SH)(OPh)$ (**3**). In solution at room temperature, $[L^{Pr}MoOS(OPh)]^-$ displays a broad isotropic EPR signal with $\langle g \rangle$ 1.9248 while **3** exhibits a sharp doublet resonance with $\langle g \rangle$ 1.9480 and A_H 11.3 $\times 10^{-4}$ cm^{-1}. Frozen glass EPR spectra of both complexes exhibit a sharp, anisotropic signal, with g_1 2.0029, g_2 1.9283, and g_3 1.8529, which is assigned to $[L^{Pr}MoOS(OPh)]^-$. Under anaerobic conditions, these Mo(V) species are stable for many days.

Reaction of **1** with $CoCp_2$ in toluene results in the precipitation of light-brown $CoCp_2[L^{Pr}MoOS(OPh)]$ (**4**).[16,17] The compound is moderately stable in the solid state and stable for days in anaerobic, anhydrous acetonitrile solutions. Its solid-state and solution EPR spectra are identical to those of $[L^{Pr}MoOS(OPh)]^-$ generated in situ. In the presence of H_2O, solutions of **4** exhibit a second EPR signal characteristic of **3**. The IR spectrum of **4** is consistent with the formulation. The complex exhibits a strong pre-edge feature in its S K-edge XAS, consistent with the presence of the Mo^V═S unit. This contrasts with the findings of Singh et al.[18] concerning the nature of the thio group in $PPh_4[(L\text{-}N_2S_2)Mo^VOS]$ ($L\text{-}N_2S_2$ = *N*,*N*′-dimethyl-*N*,*N*′-bis(2-mercaptophenyl)ethylenediamine).

Complex **1** reacts with NEt_4CN in acetonitrile to produce $L^{Pr}MoO(MeCN)(OPh)$ and SCN^-. When the reaction is performed in air using wet solvents, $L^{Pr}MoO_2(OPh)$ and SCN^- are produced, the overall reaction modeling the deactivation of the molybdenum hydroxylases by cyanide.[2,3] In acetonitrile, **1** reacts with PPh_3 to form $L^{Pr}MoO(OPh)(MeCN)$ and $SPPh_3$ (established by ^{31}P NMR). Nucleophilic attack of the thio group is consistent with relative Mo═O and Mo═S π* orbital energies and previous studies.[3,4] This behavior is in accord with the general view that an aqua/hydroxo ligand, rather than an oxo ligand, is transferred during enzyme turnover.[2,3] The susceptibility of $[L^{Pr}MoOS(OPh)]^-$ to protonation parallels the behavior of the "Very Rapid" center.[2,5]

This paper describes the first molybdenum hydroxylase model to feature interconvertible, monomeric $[Mo^{VI}OS]^{2+}$ (**1**), $[Mo^VOS]^+$ (**4**), and $[Mo^VO(SH)]$ (**3**) complexes possessing biologically relevant structural, spectroscopic, and chemical properties. These complexes constitute individual models for the oxidized, active enzyme and the "Very Rapid" and "Rapid" Mo(V) states, respectively. Our work to date provides a solid foundation for the development of a comprehensive model for the molybdenum hydroxylases. Future work will fully define the chemistry of these and related complexes, and explore the possibility of developing systems featuring the crucial water-based co-ligand and substrate reactions of the natural systems.

Acknowledgment. We thank Mr. C. Doonan for EPR experiments and gratefully acknowledge the financial support of the Australian Research Council. SSRL is funded by the Department of Energy (DOE) BES, with further support by DOE OBER and the NIH.

Supporting Information Available: An X-ray crystallographic file (PDF). An X-ray crystallographic file in CIF format. This material is available free of charge via the Internet at http://pubs.acs.org.

JA9938332

(15) Mo K-edge EXAFS fits. **2**: 1 Mo═O at 1.693(1) Å, σ^2 (Debye−Waller factor) 0.0018(3) Å^2; 1 Mo−S at 2.324(1) Å, σ^2 0.0019(3) Å^2; 1 Mo−O at 1.929(2) Å, σ^2 0.0034(4) Å^2; 3 Mo−N at 2.268(2) Å, σ^2 0.0062(12) Å^2; 1 Mo···S at 3.462(4) Å, σ^2 0.0031(3) Å^2; 1 Mo···Mo at 5.584(4) Å, σ^2 0.0039(4) Å^2. **1**/toluene: 1 Mo═O at 1.695(2) Å, σ^2 0.0025(3) Å^2; 1 Mo═S at 2.155(4) Å, σ^2 0.0034(4) Å^2; 1 Mo−O at 1.962(2) Å, σ^2 0.0023(3) Å^2; 3 Mo−N 2.289(3) Å, σ^2 0.0064(9) Å^2.

(16) For analogous syntheses of $CoCp_2[L^xMoO_2(SPh)]$ see: Xiao, Z.; Gable, R. W.; Wedd, A. G.; Young, C. G. *J. Am. Chem. Soc.* **1996**, *118*, 2912−2921.

(17) A solution of cobaltocene (189 mg, 1 mmol) in dry, deoxygenated toluene (10 mL) was added with rapid stirring to **1** (289 mg, 0.5 mmol). After stirring for 15 min, the light brown precipitate was isolated by anaerobic filtration, washed with toluene (2 × 5 mL), hexane (2 × 5 mL), and vacuum-dried. Anal. Calcd for $C_{34}H_{43}BCoMoN_6O_2S$: C, 53.34; H, 5.80; N, 10.85; S, 4.15. Found: C, 52.81; H, 5.73; N, 10.85; S, 4.15. IR (KBr, cm^{-1}) ν(CN) 1509 s, ν(Mo═O) ca. 890 (m, obscured), ν(Mo═S) 440 m. UV/vis, λ/nm (ϵ/M^{-1} cm^{-1}) (MeCN) 1250 (120), 512 (435). EPR (CH_2Cl_2, 295 K) $\langle g \rangle$ 1.9248. EPR (solid, 295 K) g_1 1.9992, g_2 1.9243, g_3 1.8491.

(18) Singh, R.; Spence, J. T.; George, G. N.; Cramer, S. P. *Inorg. Chem.* **1989**, *28*, 8−10.